

N74 30952

MOSSBAUER EFFECT AND ITS APPLICATIONS

IN MATERIALS RESEARCH

Jag J. Singh
Langley Research Center
Hampton, Virginia

Presented at
Symposium on Welding, Bonding, and Fastening
Williamsburg, Virginia
May 30 - June 1, 1972

641<

MOSSBAUER EFFECT AND ITS APPLICATIONS

IN MATERIALS RESEARCH

Jag J. Singh
Langley Research Center

INTRODUCTION

Mossbauer effect spectroscopic measurements provide data for a selected atom and its environments in a given matrix. The Mossbauer spectrum of a given atom, in a certain chemical environment, is unique and its characteristic parameters can be measured with a great degree of accuracy. The presence of any chemical impurities, or changes in the atomic composition of its neighborhood, will cause changes in the Mossbauer parameters. The measurement of these changes can serve as the basis for analysis of matrix variations. (See Figure 1 for a summary of various factors that can affect Mossbauer parameters.)

It is generally recognized that in any well-behaved metal fatigue failure, the following sequence of events occurs: The application of stress (cyclic or static) causes the movement of defects already present in the specimen, besides producing new defects. These defects concentrate in the regions of stress concentration. (In otherwise unflawed materials, fatigue cracks always nucleate in these regions.) This defect concentration, which precedes crack nucleation and its eventual growth, actually amounts to environmental changes for Mossbauer atoms located in these regions. These changes in the atomic composition of the Mossbauer absorber atom environment can be sensed by examining changes in the sensitive parameters

of the Mossbauer spectra. We have completed a preliminary study of changes in the isomer shift and line width of commercial nonmagnetic steel specimen. The results of this study will be discussed in this paper.

EXPERIMENTAL PROCEDURE

(a) Mossbauer Spectrometer. This study first involved the development of an efficient backscattering technique of Mossbauer spectroscopy, since the existing techniques (Refs. 1 and 2), shown in Figures 2 and 3, are either inefficient or require a specialized specimen geometry. The essential element of backscattering spectroscopy is the radiation detector. An annular detector, which would permit the collimated incident radiation to pass through to strike the test specimen located immediately behind it appears to meet the requirements of high detector-specimen solid angle as well as of in situ measurements. Such a detector has been developed and is shown in Figure 4. It consists of a 2" x 2" x 0.6" NaI(Tl) crystal, with a 0.6" diameter central hole, coupled to two matched photomultipliers. A schematic diagram of the electronic circuit for equalizing the gains and the time constants of the two multiplier channels is shown in Figure 5. This figure also shows the rest of the circuit - including the Mossbauer source motion transducer and the multichannel analyzer.

The incident beam has to be well-collimated in order to minimize the dispersion in the source-scatterer relative velocity and also to

avoid striking the radiation detector before striking the specimen (scatterer). A magnified view of the source collimator and the test specimen is shown in Figure 6. Using the dimensions given in this figure, it is easily seen that the collimator assembly keeps the incident photon beam divergence at the scatterer to an angle less than 2.5° . This low divergence reduces the source velocity dispersion at the scatterer to less than 0.1 percent.

The annular radiation counter, in combination with a stable electro-mechanical transducer and drive system producing motion of the source with constant acceleration through a range of velocities, can be used to study Mossbauer spectra in both the transmission and scattering geometries. Figures 7 and 8 show the transmission and the backscattering spectra, respectively, obtained with a 0.8 mg/cm^2 , Fe^{57} -enriched iron target. Figure 9 shows a typical backscattered Mossbauer spectrum obtained with a 0.030-inch thick nonmagnetic (SS-347) steel scatterer. The Mossbauer source in all these cases was a 10-mc Co^{57} source in platinum matrix. The absorber/scatterer in each case was positioned to subtend an angle of π steradians at the detector. From Figures 7 and 8, it is clear that the present detector configuration is capable of producing equally good transmission and backscattering Mossbauer spectra. Figure 9 clearly shows that the present system is usable with scatterers of any arbitrary thickness (Ref. 3).

(b) Metal Fatigue Damage Study. As indicated in the introduction, when a metal specimen is progressively fatigued, dislocations start

piling up in the regions of stress concentration. In the absence of stress raisers, these dislocations will be randomly distributed throughout the test specimen and will not have a significant effect in modifying the absorber atom surroundings. Following these arguments, austenite steel specimen (SS-302, SS-321, and SS-347) with stress raisers were prepared in two different geometrical configurations shown in Figure 10. Experience has shown that test specimen with these configurations develop cracks at the notches or the sharp cuts, presumably due to dislocation concentration there. These specimen were subjected to tension-tension cyclic loading in the range $2 \text{ kgm/mm}^2 \rightarrow 20 \text{ kgm/mm}^2$ at the rate of 1000 cpm and the backscattered spectra from them^(*) measured at different levels of fatigue cycles. These spectra were analyzed and the values of isomer shift, peak width, and the Mossbauer resonant fraction were computed using a program described in Ref. 4. Typical results showing the dependence of two selected Mossbauer parameters on the number of fatigue cycles in (SS-347) specimen are shown in Figure 11.

DISCUSSION

The defect/dislocation pile up in the regions of stress concentration in the test specimen leads to the creation of several nonequivalent Mossbauer absorber atom sites in the area under observation. In the

^(*) The spectra were obtained from the regions where stress raisers were located, namely, the edges of the notches or the sides adjacent to the eloxed cut.

case of point defects, it can be argued (Ref. 5) that the net result is the superposition of several modified Mossbauer frequencies, ω' :

$$\omega' = \omega_0 + \sum_{lm} a_{lm} \omega_{lm} \quad (1)$$

where ω_0 = undisturbed Mossbauer frequency

a_{lm} = concentration of defects of type m at l

ω_{lm} = frequency shift caused by the defects of type m at l
 $= \alpha_{ij}^m U_{ij}(-r_l)$

where α_{ij}^m stands for the deformation tensor relating the frequency change and the deformation potential,

$U_{ij}^m(-r_l)$.

This statistical summation should result in widening the Mossbauer peak and also changing the isomer shift. The effects of point defects and dislocations on line widths - in limiting cases - are expected to be of the following form (Ref. 5):

$$\left. \begin{aligned} \tau &\propto (N_d)^{1/2} \\ &\text{for } \ln N_d \gg 1 \\ \tau &\propto (N_d^0) \\ &\text{for } N_d^0 R^2 \ll 1 \end{aligned} \right\} \quad (2)$$

where N_d = linear dislocation density

N_d^0 = dislocation loop density

and R = characteristic dimension of the dislocation loop.

Thus, one expects the Mossbauer parameters to continue to change with the fatigue cycles till a nucleus of the crack has been formed. This change is expected to be of the "saturation" type since the later dislocation development will have reduced effect in creating additional nonequivalent sites or lattice distortion. The "saturation" change can be related to the critical stage of the specimen when crack nucleation is imminent.

An examination of Figure 11 shows that the peak width shows a distinct upward trend with the increasing number of fatigue cycles whereas the isomer shift is barely affected. This may be interpreted to indicate that quadrupole splitting is playing a role. However, the specimen were commercial, polycrystalline steels of ill-defined history and detailed measurements on single crystal specimen should be made before any firm conclusions can be drawn (Ref. 6). It does appear, however, that the changes in the Mossbauer parameters with fatigue are small and the use of W^{181} as the Mossbauer source may be more appropriate. (This stems from the long half life, Ref. 7, of Ta^{181} (6.25 keV) state, leading to a natural line width of 3.2×10^{-3} mm/sec compared with 0.197 mm/sec for Fe^{57} .) Ta^{181} , which can be diffused into the material under study will have a tendency to go to the grain boundaries where dislocations also tend to concentrate.

REFERENCES

1. Mossbauer Effect Methodology, Vol. I, edited by I. J. Gruverman. Published by Plenum Press, 1965.
2. K. R. Swanson and J. J. Spijkerman: J. Appl. Phys. 41, 3155, 1970.
3. J. J. Singh: Nucl. Instr. & Meth. (to be published) and NASA TN D-6819, 1972.
4. L. M. Howser, J. J. Singh, and R. E. Smith, Jr.: NASA TM X-2522, 1972.
5. L. B. Kvashnina and M. A. Krivoglaz: Fiz. Metal. Metalloved, 23, 1967.
6. J. J. Singh: Bull. Am. Phys. Soc., 17, 547, 1972.
7. Tables of Isotopes (6th Edition), edited by C. M. Lederer, J. M. Hollander, and I. Perlman. Published by John Wiley and Sons (1967).

Applications Of Mossbauer Spectroscopy To Physical Metallurgy Are Based On The Following Factors :

- (1) NEIGHBORING ATOM INTERACTIONS.**
- (2) LOCAL CUBIC SYMMETRY.**
- (3) ELECTROSTATIC (QUADRUPOLE) INTERACTIONS.**
- (4) LATTICE DISTORTION (POLYCRYSTALLINE ALLOYS)**

CHANGES IN THESE FACTORS, RESULTING FROM DISLOCATION MOVEMENTS AND PILE UP, AFFECT THE INTERNAL MAGNETIC FIELD, THE ISOMER SHIFT, THE ELECTRIC FIELD GRADIENT AND THE LATTICE PARAMETERS AT THE ABSORBER ATOM SITES. THESE CHANGES MAY BE MORE PRONOUNCED IN MATERIALS WITH LOW STACKING FAULT ENERGIES.

FIGURE 1

649<

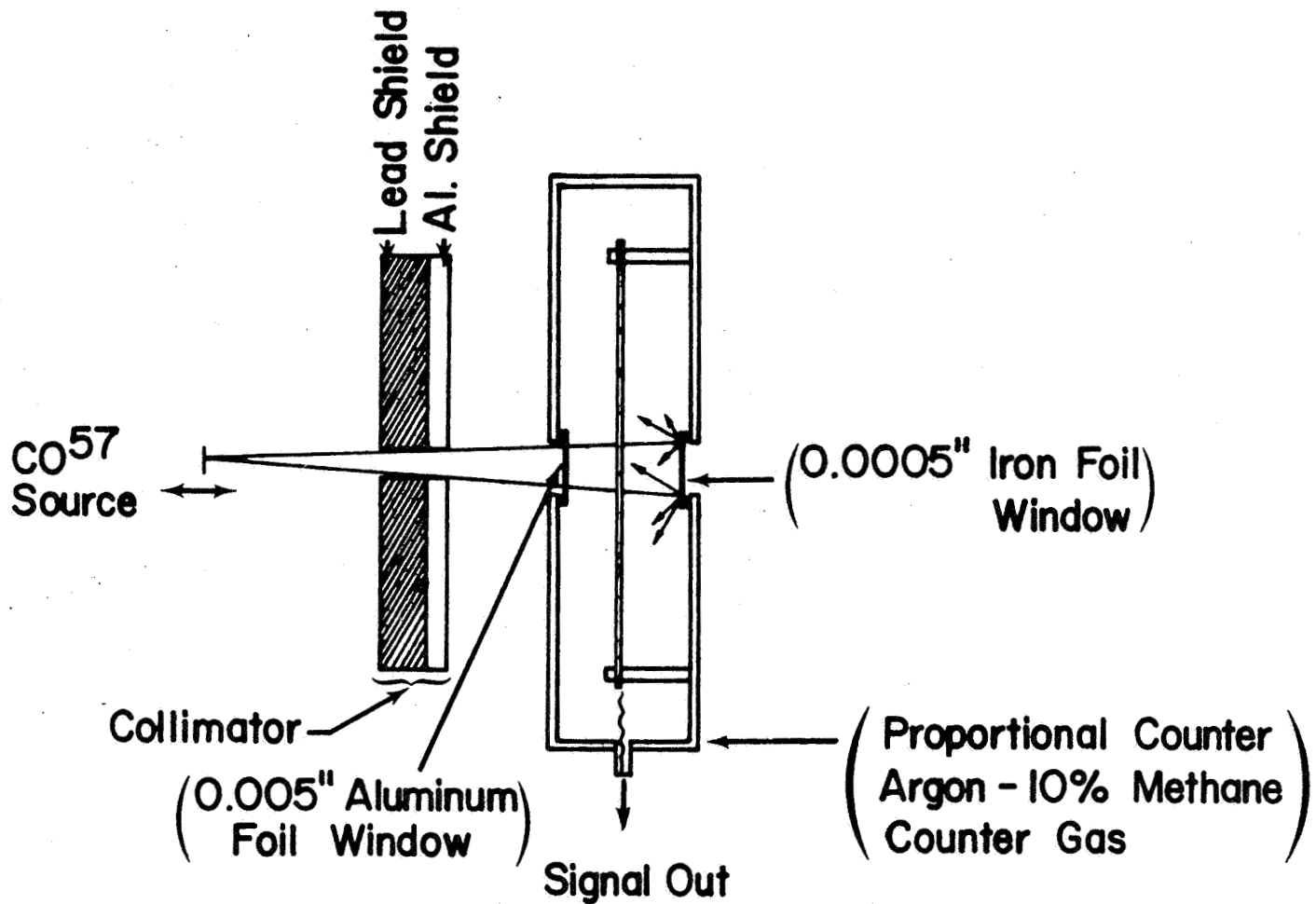


Figure -2. Schematic Arrangement for Scattering Geometry ($\bar{\epsilon}$ - Counting) in Mossbauer Spectroscopy.

FIGURE 2

650<

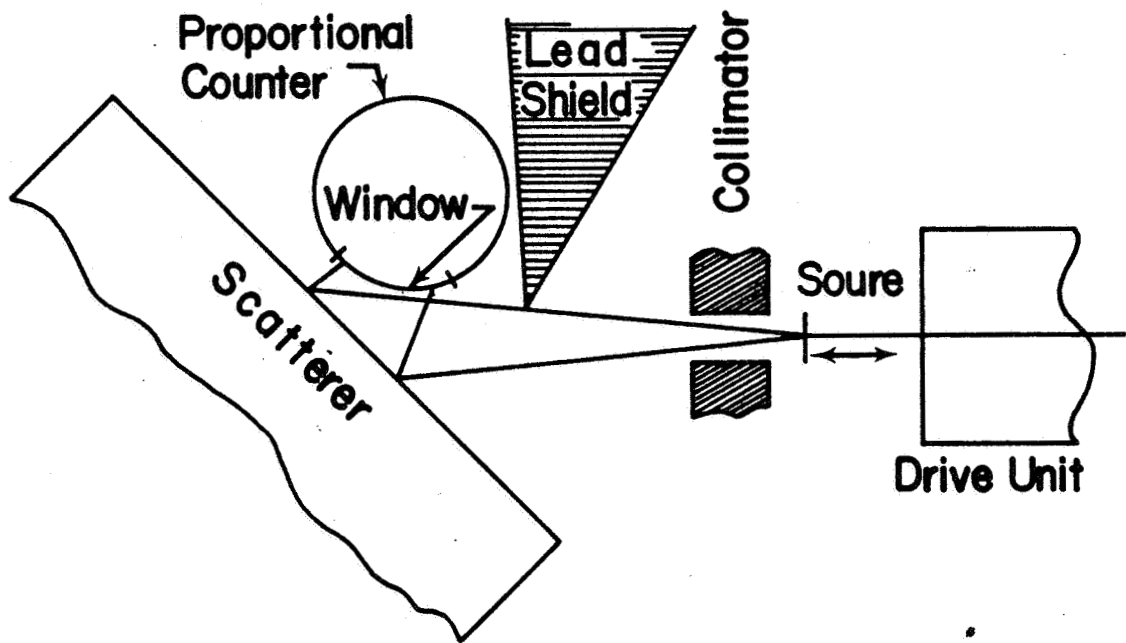
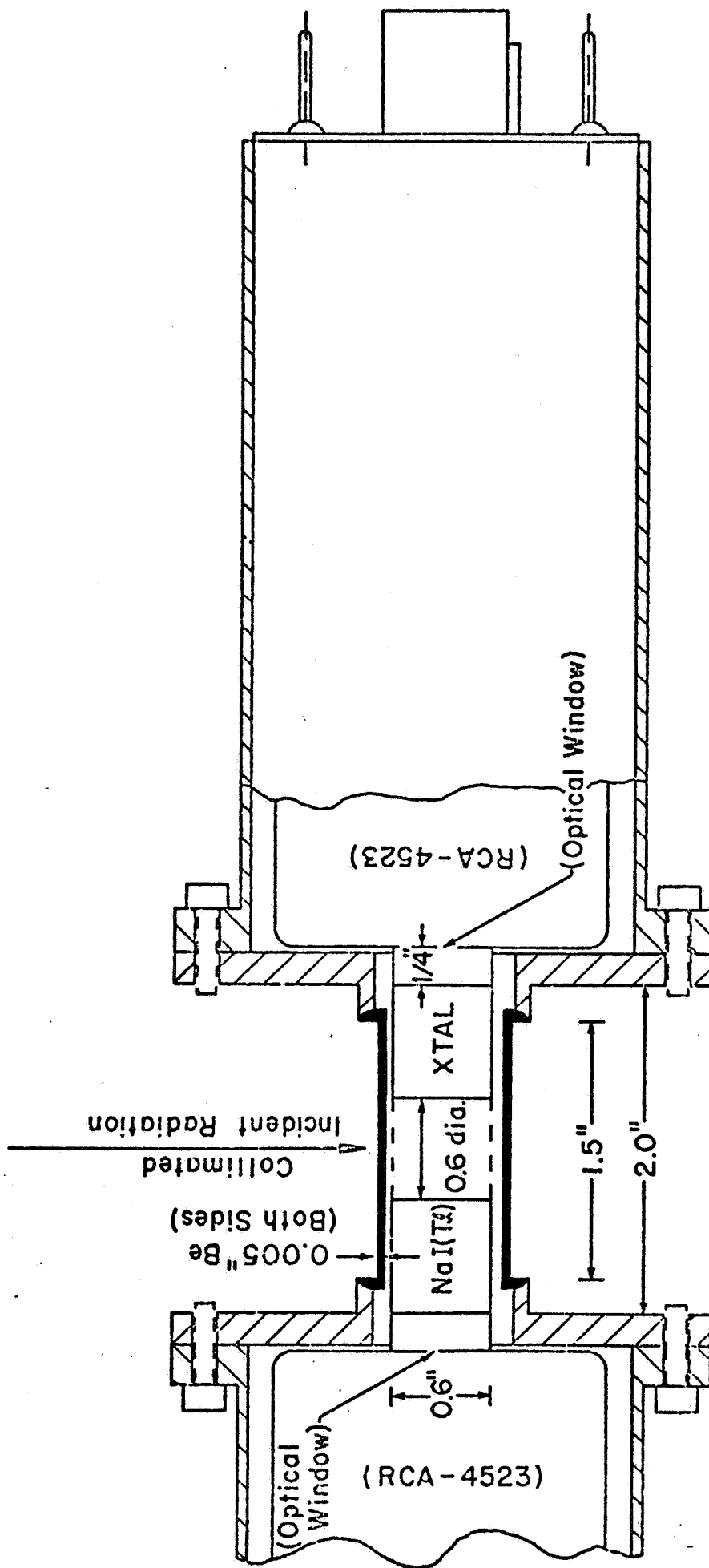


Figure -3. Schematic Arrangement for Scattering Geometry (Photon Counting) in Mossbauer Spectroscopy.

FIGURE 3

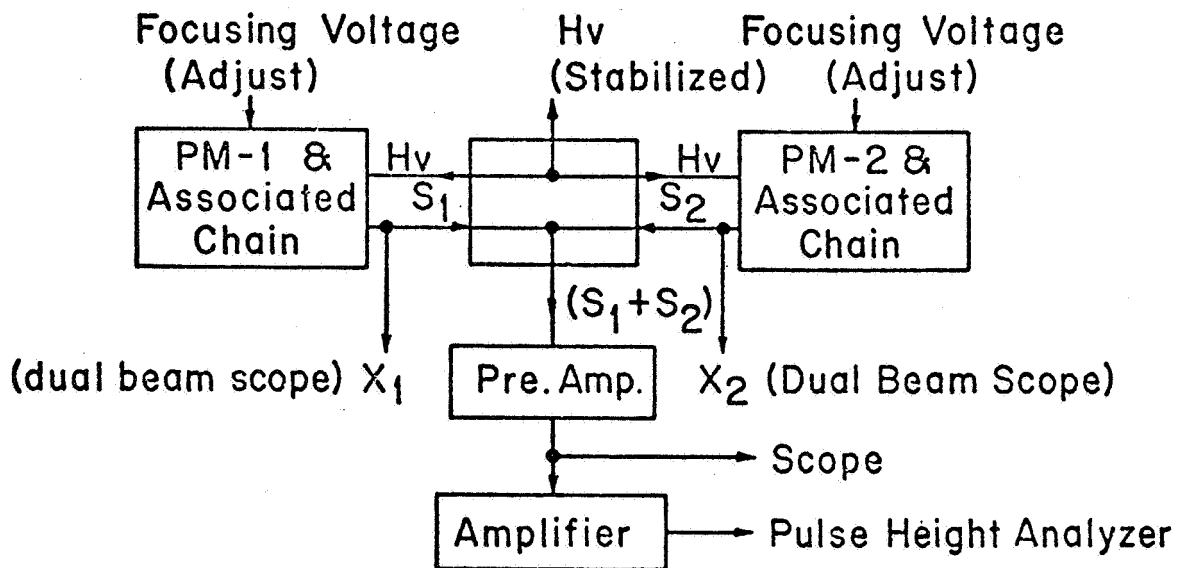
651<



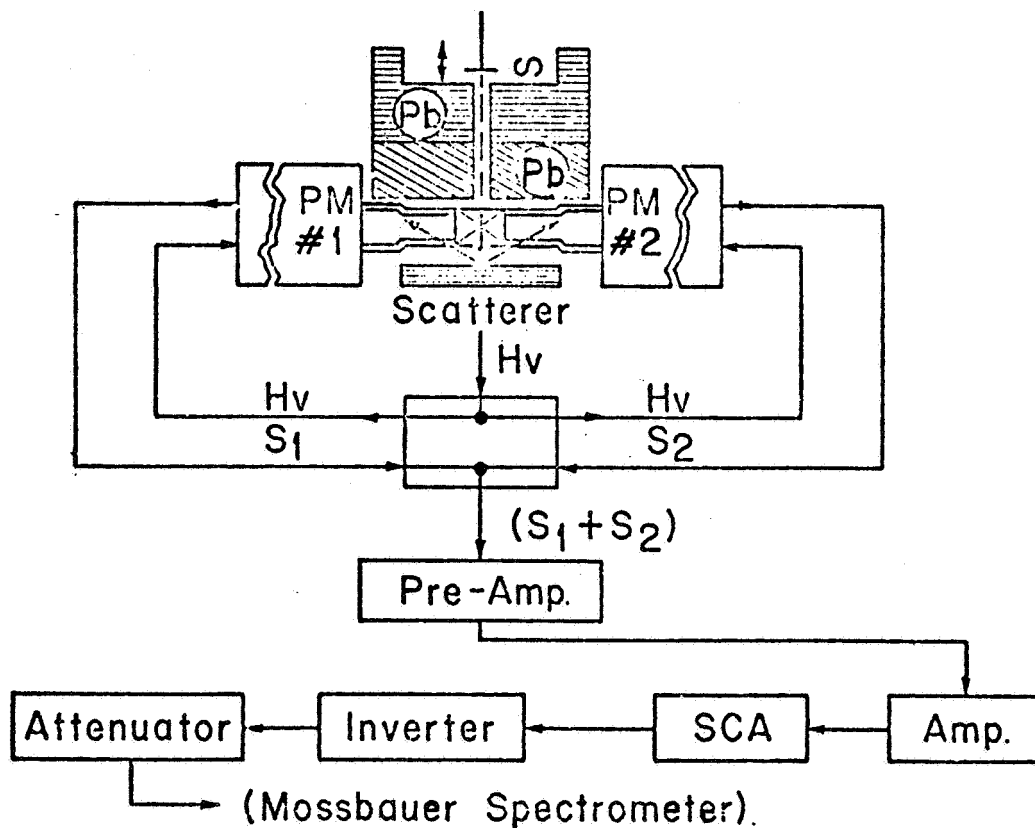
652

Schematic Drawing of the (0.6" X 2" X 2") Annular NaI (Tl) Detector Assembly.
 (Notice the 0.005" Beryllium Windows on Both Sides.)

FIGURE 4

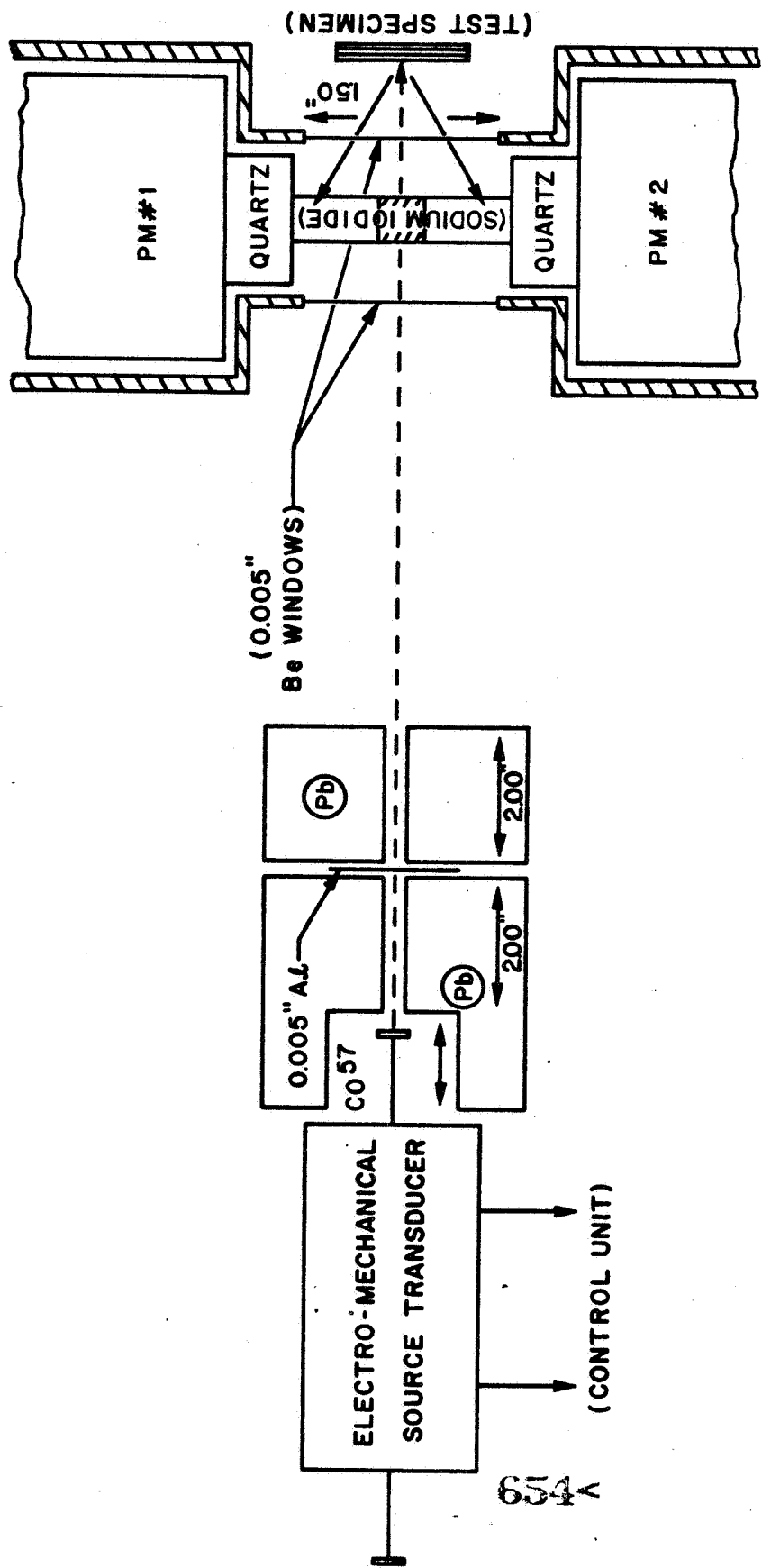


General Circuit for Equalizing Photomultiplier Gains and Pulse Arrival Times.



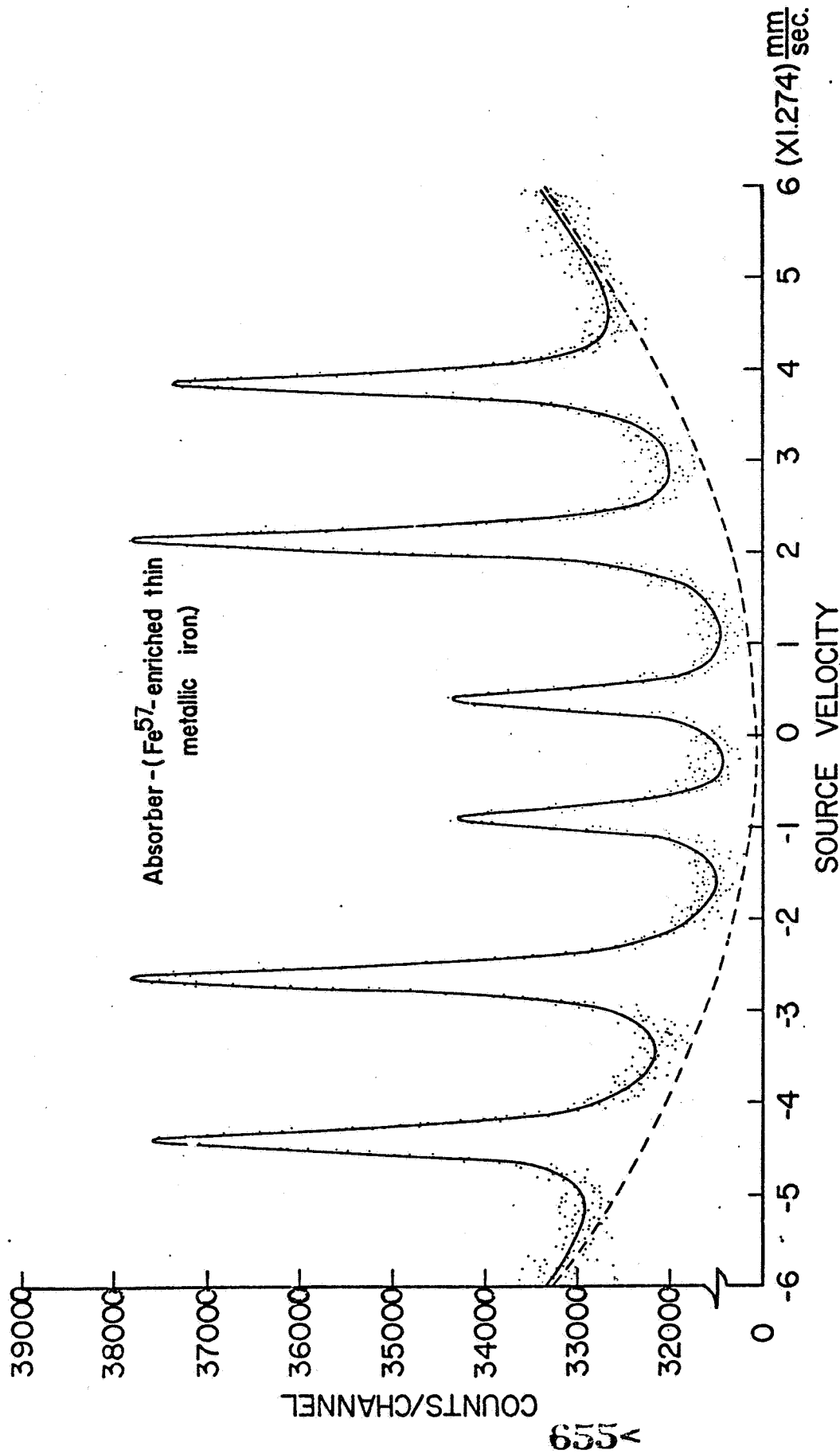
Schematic Diagram of the Signal Conditioning Circuit for Mossbauer Spectrometer.

FIGURE 5



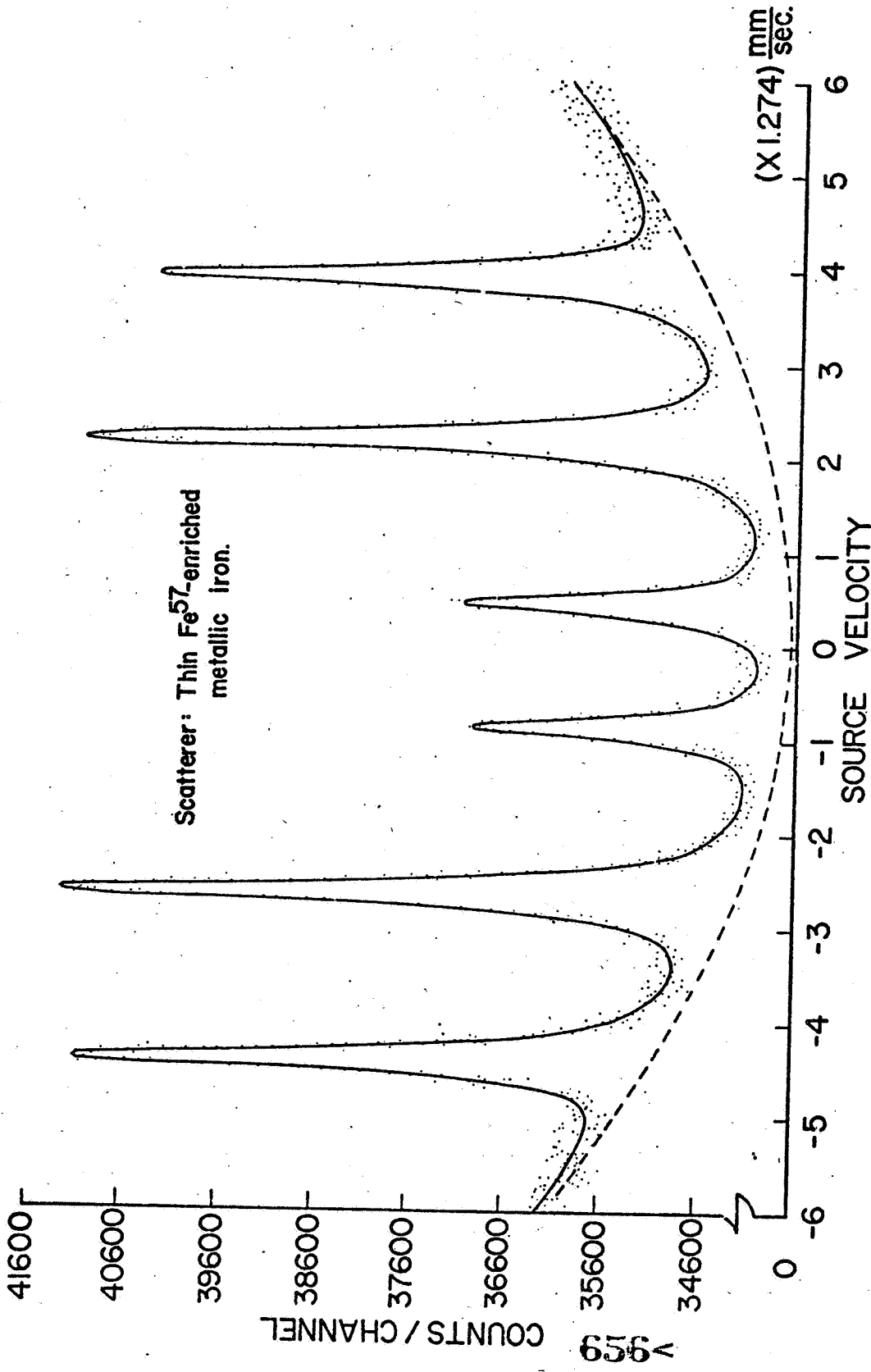
EXPERIMENTAL SET-UP FOR MES INSPECTION.

FIGURE 6



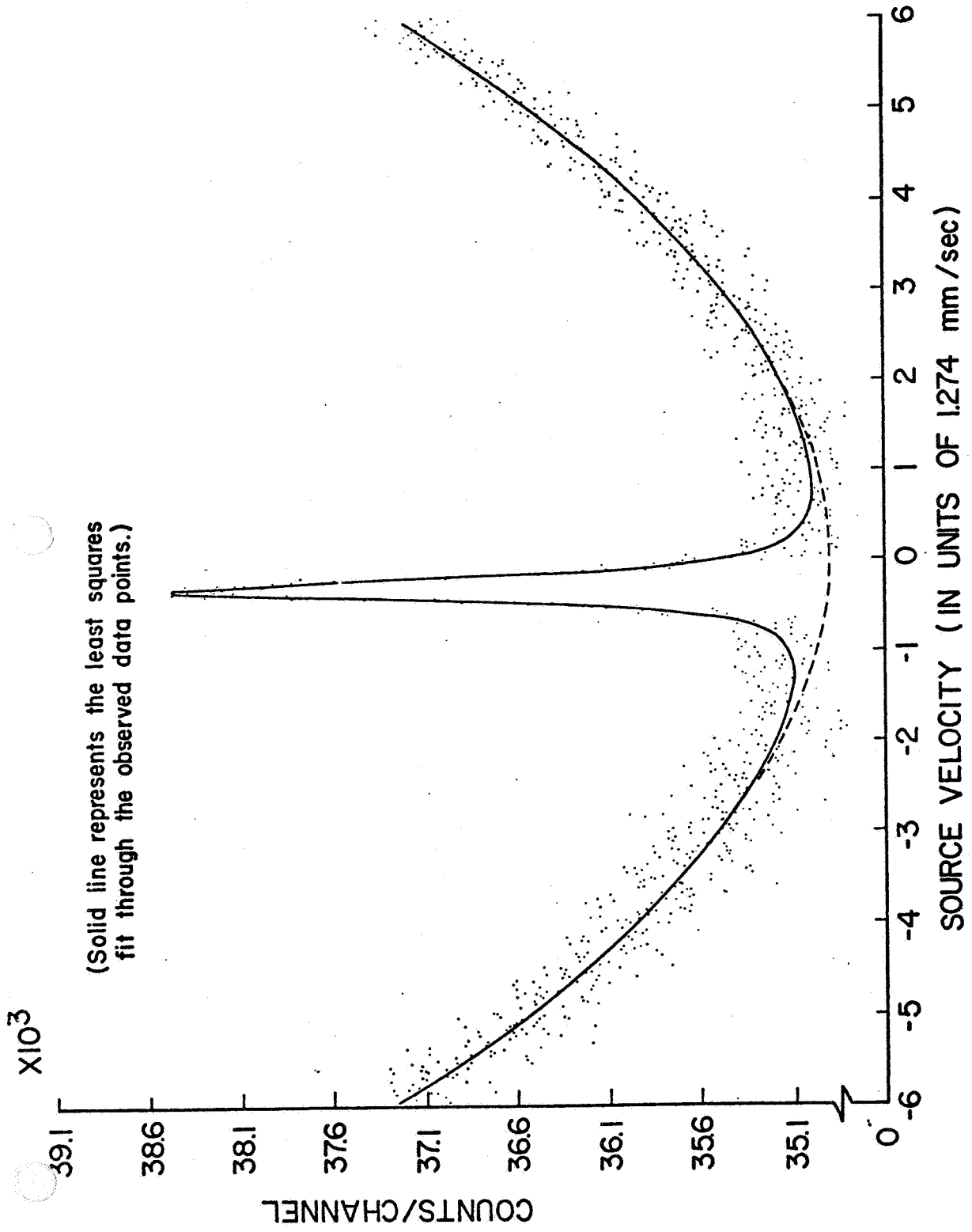
A Typical Transmission Spectrum from a Thin (0.8 mg/cm²) Fe⁵⁷-Enriched Iron Absorber with the Langley Detector. (Notice the Characteristic Scattering 'Peaks' Instead of the Transmission 'Dips'.)

FIGURE 7



A Typical Backscattering Spectrum from a thin (0.8 mg/cm²) Fe⁵⁷-enriched iron Scatterer with the Langley Detector. (Notice the pronounced Scattering Peaks Characteristic of Scattering Geometry.)

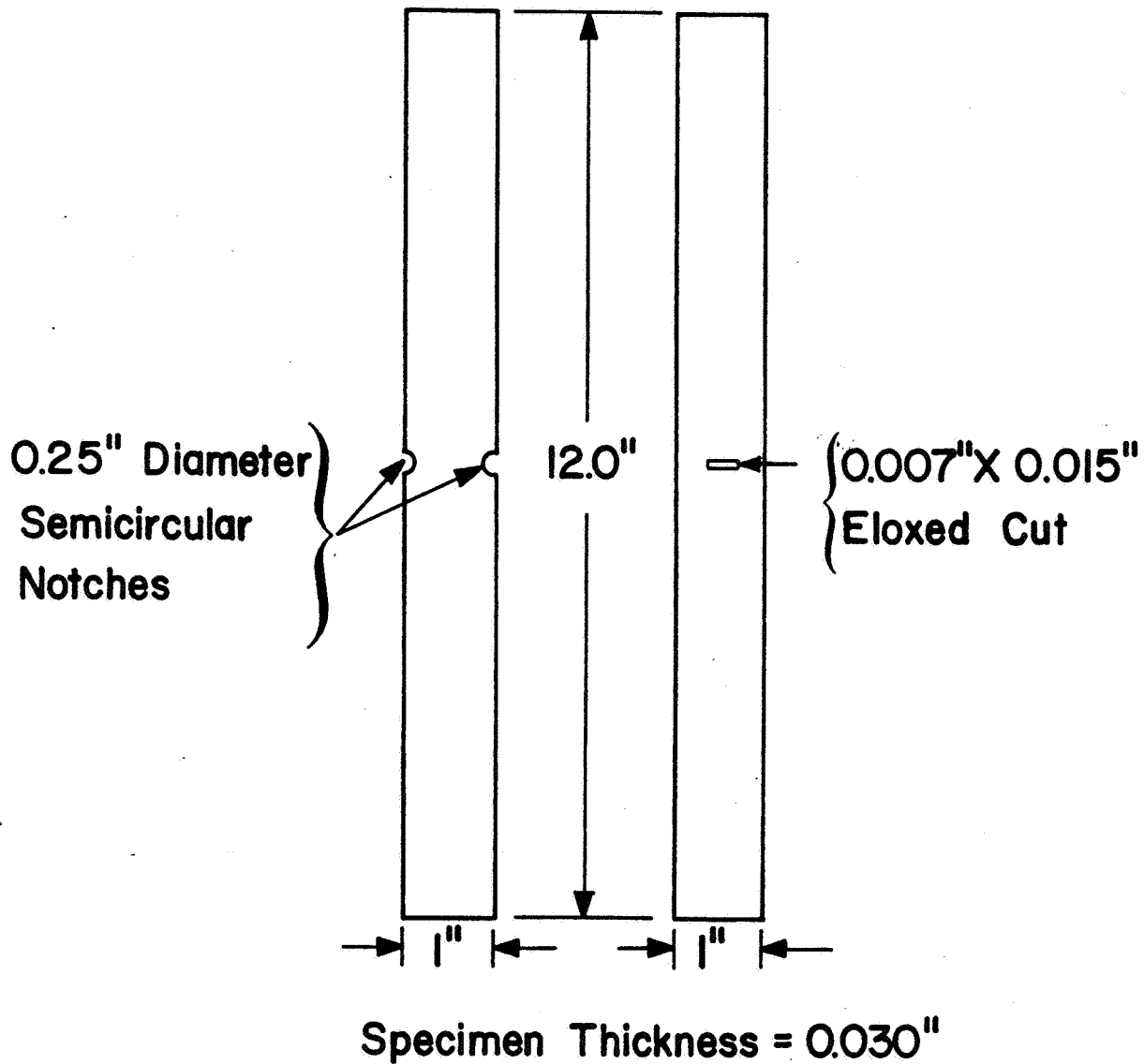
FIGURE 8



V 759

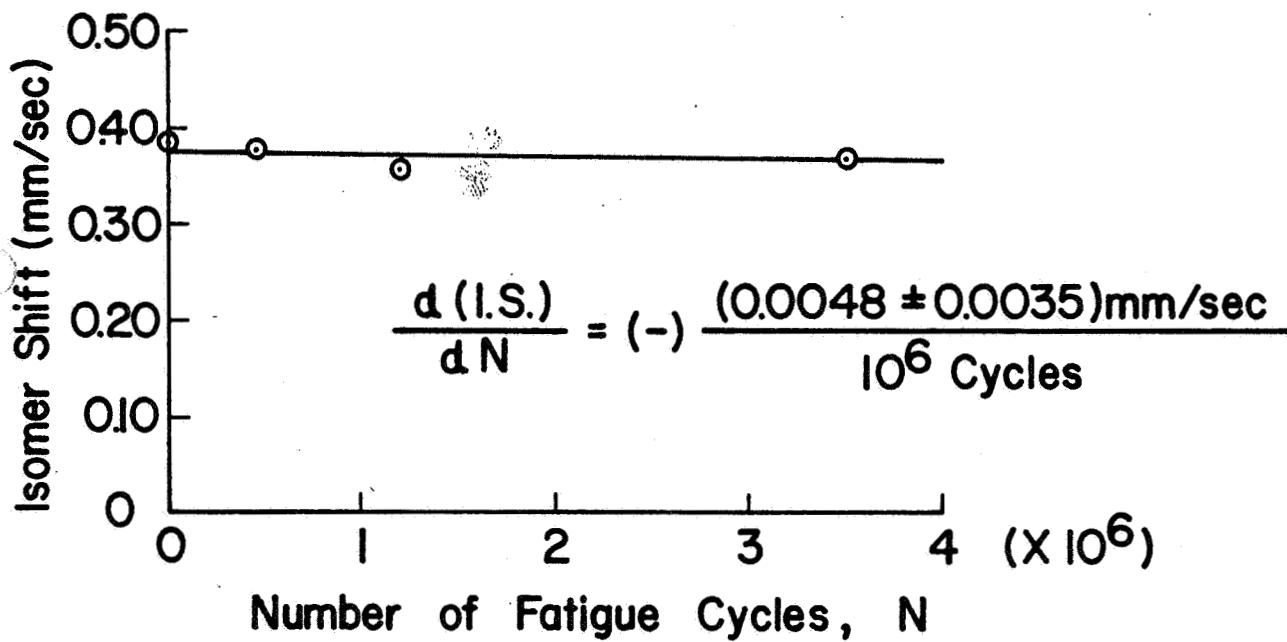
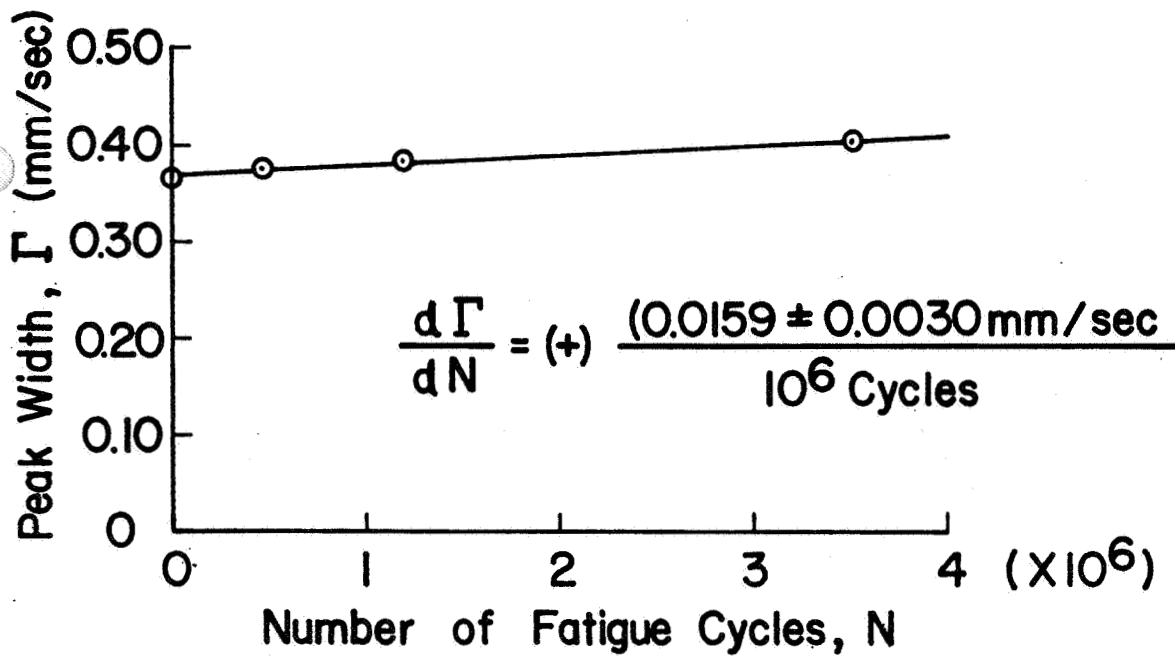
Backscattered Spectrum from a (SS-347) Steel Specimen Using the Radiation Detector Described in this Paper.

FIGURE 9



Geometrical Configurations of Steel Specimen used in the Study of Fatigue-induced changes in their Mossbauer Spectra.

FIGURE 10



Dependence of Mossbauer Peak Width (Γ) and Isomer Shift (I.S.) on Cyclic Stress in SS-347 Steel Specimen.

FIGURE 11
659<